

Effect of Al Antioxidant on the Rate of Oxidation of Carbon in MgO–C Refractory

S. K. Sadrnezhaad,[†] Z. A. Nemati, S. Mahshid, S. Hosseini, and B. Hashemi

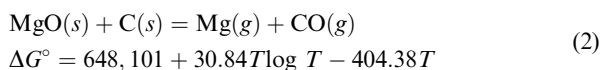
Center of Excellence for Production of Advanced Materials, Department of Materials Science and Engineering, Sharif University of Technology, Tehran 11365-9466, Iran

Kinetics of air oxidation of MgO–C–Al refractory at 600°–1300°C were investigated using the software based on the modified shrinking core model (KDA). Commercial bricks containing 88.5% MgO, 10% residual carbon, and 1.5% aluminum antioxidant were oxidized isothermally with air. Combination of experimental data with model calculations indicated gas diffusion through solid material and pores as a major controlling step. Previously observed chemisorption process was eliminated from the rate-controlling mechanism with addition of aluminum antioxidant. Comprehensive rate equations were devised for MgO–C–Al and MgO–C oxidation reactions. Overall activation energies of Q_{id} (internal diffusion) = 139.15 kJ/mol at $T \leq 800^\circ\text{C}$ and Q_{pd} (pore diffusion) = 25.48 kJ/mol at $T > 800^\circ\text{C}$ were obtained for MgO–C–Al oxidation reactions. Corresponding values were determined to be $Q_{id} = 134.85$ kJ/mol and Q_{ca} (chemical adsorption) = 66.69 kJ/mol at $T \leq 800^\circ\text{C}$ and $Q_{pd} = 18.95$ kJ/mol and $Q_{ca} = 66.69$ kJ/mol at $T > 800^\circ\text{C}$ for MgO–C oxidation reactions. Addition of aluminum antioxidant indicated a reducing effect on oxidation of MgO–C bricks at $800^\circ\text{C} \leq T \leq 1250^\circ\text{C}$. Reverse behavior was observed at $T \leq 700^\circ\text{C}$.

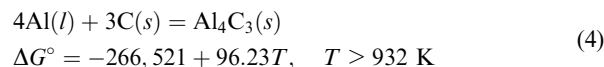
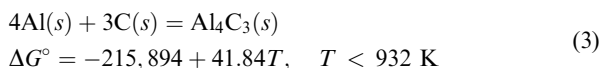
I. Introduction

THE MgO–C refractories with and without antioxidants are substantially used in iron and steel industries. Their role in basic oxygen furnace (BOF), electric arc furnace (EAF), and ladle metallurgy (LF) has grown exponentially in recent years. Combination of graphite with MgO increases resistance to thermal shock, controls thermal expansion, improves corrosion resistance, and decreases wettability with corrosive liquid phases. High-temperature oxidation is, however, a major drawback that reduces MgO–C brick performance.¹

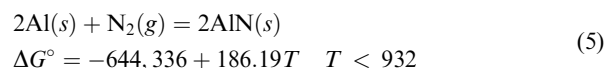
Two oxidation mechanisms are discussed for MgO–C bricks in the literature^{1,2}: (a) direct oxidation at temperatures lower than 1400°C according to Eq. (1) and (b) indirect oxidation at temperatures higher than 1400°C according to Eq. (2)¹:



Aluminum can react with graphite flakes to form compounds that affect the behavior of the refractory substances^{3,4}:



Other reactions may also occur to change the oxidation behavior of the refractory brick to lower rates:



The effect of aluminum antioxidant on the formation of Al_4C_3 , $\text{AlN}(s)$, $\text{Al}_2\text{O}_3(s)$, and $\text{MgO} \cdot \text{Al}_2\text{O}_3(s)$ spinel at 1200° and 1500°C has been studied by Yamaguchi.⁵ He found that aluminum vapor diffuses through the refractory material, reacting with carbon and N_2 to form $\text{Al}_4\text{C}_3(s)$ and $\text{AlN}(s)$ whiskers, respectively. These processes plus the formation of $\text{MgO} \cdot \text{Al}_2\text{O}_3(s)$ spinel result in great morphological change and reduction of the oxidation rate.⁴ The effects of oxygen and nitrogen partial pressures on the stability of different phases present in carbon-containing refractories were also studied by Yamaguchi^{5,6} and Poirier and Rigaud.⁷ The effect of MgO grain size and graphite content on the physical and chemical properties of MgO–C substances has also been extensively investigated.^{8–11} Kinetics of oxidation of an antioxidant containing MgO–C masses, however, need to be investigated in greater depth.

Carniglia¹² and Tabata *et al.*¹³ studied the reactions between MgO and C at temperatures greater than 1400°C. Ichikawa *et al.*¹⁴ studied the kinetics of direct oxidation of carbon present in MgO–C bricks at 1000°C. Ghosh *et al.*¹⁵ studied the oxidation mechanism of graphite in MgO–C bricks at temperatures between 800° and 1200°C by isothermal weight-loss measurements. They reported a diffusion mechanism with an activation energy of 20.9 kJ/mol.

Faghihi-Sani and Yamaguchi¹⁶ reported a two-stage model for the direct oxidation mechanism of graphite at temperatures between 1000° and 1200°C. They proposed a pore diffusion—film transfer mechanism having activation energies of 49.47 kJ/mol and 46.63 kJ/mol, respectively. Li *et al.*¹⁷ studied direct oxidation of refractory carbon in the temperature range of 1000°–1400°C. They determined the reaction rates by measuring the CO content of the exhaust gas that converted to CO_2 . They reported an activation energy of 48.46 kJ/mol for graphite oxidation.

Both values given by the above authors for film transfer and pore diffusion mechanisms seem to be much larger than the values generally accepted for these regimes.^{1,18} The activation energies reported by Faghihi-Sani *et al.*¹⁶ and Li *et al.*¹⁷ are much greater than the activation energy of 20.9 kJ/mol reported for 800°–1200°C by Ghosh *et al.*¹⁵ A combination of chemical adsorption with pore diffusion of the gases within the decarburized layer showed a better fit at corresponding temperatures studied later.¹

Table I. Chemical Composition of Sintered Magnesia and Graphite Ash

Composition (wt%)	MgO	Al ₂ O ₃	SiO ₂	CaO	Fe ₂ O ₃	LOI
Synthetic sample	97.1	1.26	0.56	0.09	0.89	0.01
Industrial brick	97.5	0.2	0.5	1.2	0.5	0.1
Graphite ash	7.67	17.10	50.20	5.06	17.81	Na ₂ O: 0.79 K ₂ O: 1.37

The effect of anti-oxidants on the kinetics of oxidation of MgO–C–Al refractories in the temperature range from 800° to 1250°C is discussed in this paper. The experimental method consists of frequent weight-loss measurements on samples maintained at a constant temperature. Model calculations carried out for constant-size particles reacting with gas^{19,20} showed the mechanism and kinetic parameters of the reactions. Software developed according to the shrinking core-progressive conversion regime discussed in Sadrezhaad *et al.*¹ was used for calculations. The variation of oxidation rate with grain size was also investigated with the aim of increasing the lifetime of the refractory bricks.

II. Experimental Procedure

(1) Sample Preparation

Cylindrical refractory samples containing 10% total carbon (from graphite and phenolic resin) were produced by unidirectional die pressing at 120 MPa of a mixture of Chinese sintered magnesia and Chinese graphite flakes. Magnesia grains had 3.51 g/cm³ bulk density, 97% purity, and a maximum grain size of 5 mm. Graphite flakes contained 5 wt% ash and had a maximum grain size of 0.4 mm. Five weight percent Novolac liquid phenolic resin was added as a binder. The samples had a diameter of 30 mm and a height of 25 mm. They were cured at 240°C for 24 h. The chemical composition of magnesia and graphite is indicated in Table I. Other specifications of the raw materials used to make experimental probes are given in Table II. Their density and apparent porosities were evaluated by kerosene soaking for 24 h according to the DIN-51065 standard. They were heated again at 600°C for 5 h in a coke bed to remove the volatile species. Their apparent porosity was 12.2% after curing at 240°C and 13.4% after curing at 600°C.

Commercial refractory bricks of similar shape and chemical composition were produced by a 202 MPa hydraulic press and cured at 240°C for 24 h. They were sliced into cylindrical probes with the same dimensions as the laboratory ones. Their density and apparent porosities were evaluated in the laboratory by kerosene soaking for 24 h according to the DIN-51065 standard. They were heated at 600°C for 5 h in a coke bed to remove the volatile species. They contained 10% total carbon (from graphite and resin) and 1.5% aluminum antioxidant. Their apparent porosity was 4.3% after curing at 240°C and 7.3% after curing at 600°C.

Table II. Specification of the Raw Materials Used in this Research

Raw material	Size distribution (mm)	wt% (each size or total)
Sintered magnesia (Andreasen coefficient = 0.3)	3–5	12.07
	2–3	8.33
	1–2	12.16
	0.1–1	26.18
	<0.1	26.26
Total wt%	0–5	85
Sintered magnesia for industrial samples	1–4	42.50
	<1	24.56
	Fine powder	17.94
Phenolic resin	—	5%

Based on the experimental results, the apparent porosities of the laboratory samples are higher than those of the commercial ones. The difference seems to be due to the higher pressure of the industrial press as compared with the laboratory unit, difference in size distribution of the raw materials used, and the presence of aluminum in commercial samples. It was observed that the apparent porosities of the probes increase with temperature, whether they contain an aluminum antioxidant or not. The apparent porosities of the samples containing aluminum increase with a slower slope than that of the samples containing no antioxidant at temperatures below 1250°C. These results are consistent with those given by previous researchers.²¹

According to Uchida and Ichikawa,²² Al₄C₃(s) is practically produced above 750°C. Curing at 600°C, therefore, does not seem to cause a reaction of aluminum with carbon. Neither does it seem to oxidize during curing treatment, because embedding within the coke bed prevents any oxygen interference. The amount of resin added to MgO–C samples is not necessarily the same as that used by different researchers.^{1,4,15,23,24} Several authors have used, for example, 5% resin.^{1,15} Others have used 4%²³ or 3%.^{4,24} Investigation of the effect of resin content on the porosity of the sample is beyond the scope of this research. All samples were, thus, prepared by using 5% resin. The porosity of the samples depended on various parameters. Pyrolysis affected, for example, the porosity of the sample. This change appeared, however, due to exhausting of the volatile matter. Carbon burnout was not expected to occur, because the samples were placed in a coke bed before being heated.

(2) Oxidation Tests

Isothermal oxidation of refractory probes was carried out at different temperatures from 600° to 1300°C for 5.4 ks. A tubular furnace allowing natural convection of air and having a digital balance, which was located under the furnace, were used for weight-loss measurements. The setup was similar to that described in Sadrezhaad *et al.*¹ Weight-loss data were used for kinetic model calculations for prediction of the mechanism of the oxidation reaction with and without an aluminum antioxidant.^{19,20} Each sample was placed on an alumina tube. The tube was gradually raised in 2–3 min up in order to insert the sample into the furnace. The weight loss corresponding to this stage was neglected.

A schematic representation of the cross-sectional area of the oxidizing sample placed inside the heating furnace for weight-loss measurements is demonstrated in Fig. 1. For unidirectional oxidation from the periphery toward the center line of the sample, its top and bottom sides were covered by two pieces of alumina plates. Axial diffusion of oxygen was thus prevented from top or bottom into the sample. The weight change in the brick was measured against time. The fractional weight loss (x) was calculated based on the following definition:

$$\text{Fractional weight loss} \equiv x = \frac{\text{Weight loss at time } t}{\text{Total weight loss after complete oxidation}} \quad (6)$$

X-ray diffraction (XRD) patterns of the samples were determined by a Bruker AXS D8 Advance (D-76187, Karlsruhe, Germany) X-ray diffractometer using CuK α radiation ($\lambda = 1.5405 \text{ \AA}$).

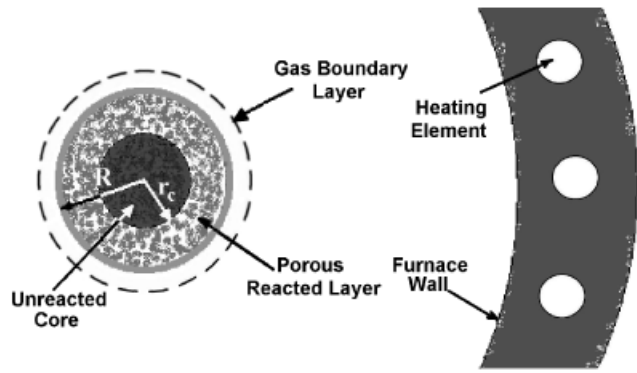


Fig. 1. Schematic representation of the cross-sectional area of the oxidizing sample placed inside the heating furnace for weight-loss measurements.

III. Results and Discussion

Figure 2 compares the sectional areas of partially oxidized probes at different temperatures. A non-oxidized core and a totally oxidized exterior shell are evident at higher temperatures ($T \geq 950^\circ\text{C}$) in both types of probes. No obvious dimensional change appears to occur during oxidation. Oxidized/non-oxidized boundary sharpness indicates internal diffusion control. Large MgO grains seem to disturb a circular reaction front at some locations within the samples. The non-circular front, however, is not expected to cause considerable error in mechanism prediction.

The constant size shrinking core model was used to predict the mechanism and kinetic parameters of the cylindrical objects.²⁵ Different stages could be recognized to develop an appropriate rate equation.¹ External mass transfer from gas to the surface of the refractory probe was found to have no influence on the oxidation rate. Inter-diffusion of gases within the porous region of the sample (pore diffusion) with a conversion time of τ_{pd} was an influential step at temperatures higher than 800°C . Gas diffusion through solid materials blocking the refractory pores with a conversion time of τ_{id} had a controlling effect at $T \leq 800^\circ\text{C}$. Chemical adsorption of gas on the graphite surface with a conversion time of τ_{ca} had a minor effect on MgO-C oxidation at all experimental temperatures. It had, however, no effect on MgO-C-Al oxidation rate in the same temperature range. The total conversion time τ (the time required to oxidize all carbon of a brick probe) was thus cor-

related with the fractional conversion x according to the following equation¹:

$$t = \tau_{pd} \times f_{pd}(x) + \tau_{id} \times f_{id}(x) + \tau_{ca} \times f_{ca}(x) \quad (7)$$

where f is a function of fractional weight loss (x) expressed according to the geometry of the kinetic system as follows²⁶⁻²⁸:

$$f_{id}(x) = x^2, \quad \text{for plate, } T \leq 1073 \text{ K} \quad (8)$$

$$f_{pd}(x) = x + (1-x)\ln(1-x), \quad \text{for cylinder, } T > 1073 \text{ K} \quad (9)$$

$$f_{ca}(x) = x, \quad \text{for graphite flake, } 873 \text{ K} \leq T \leq 1523 \text{ K} \quad (10)$$

The prevailing mechanism was determined by verifying the validity of the corresponding function by substitution of the experimental data into Eq. (7). Mathematical calculations were performed by the software (KDA) described in Sadrezaad *et al.*¹ The total conversion times were determined for both MgO-C-Al and MgO-C refractory bricks as summarized in Table III.

Based on the total conversion times given in Table III at temperatures up to 800°C , internal diffusion in solid materials is the prevailing step in both aluminum-containing and aluminum-free probes. This ruling step is substituted with gas diffusion in pores at temperatures greater than 800°C . A less effective rate-controlling step is also observed for oxidation of MgO-C brick at all temperatures. Based on model calculations, this step is due to a gas chemisorption process occurring at the surface of the graphite flakes.¹ It is, however, totally absent when an aluminum antioxidant is added to the refractory samples.

The chemisorption step in antioxidant-free probes is due to the small surface energy of graphite and its relatively slow bonding rate with atmospheric gas. Addition of aluminum results in the formation of metal-oxygen bonds and breaking of O-O bonds. Al and Al_2O_3 are electron acceptors and break the π bonding of C atoms by electron removal or covalent bond formation. Weakening of the π bonds of C atoms facilitates the oxygen chemisorption.²⁹ Aluminum, therefore, seems to have a catalytic effect and increases the rate of chemisorption of oxygen to the surface of graphite flakes. This property is also described in the literature.³⁰ The expedition of the chemical adsorption seems to signify the diffusion steps so much that they transform

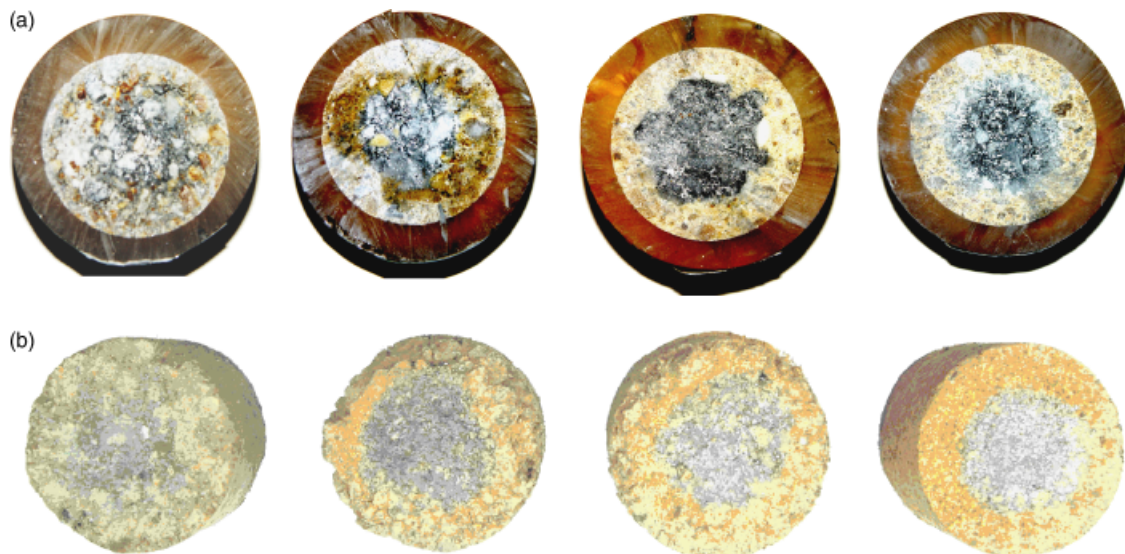


Fig. 2. Photographs of the refractory samples: (a) MgO-C-Al and (b) MgO-C oxidized from left to right at 800° , 950° , 1150° , and 1250°C , respectively. The circular ring around MgO-C-Al probes illustrates the polymeric frame used after oxidation tests to hold the samples for polishing purposes.

Table III. Total Conversion Time for Refractory Brick Oxidation Reaction: (a) MgO–C–Al and (b) MgO–C

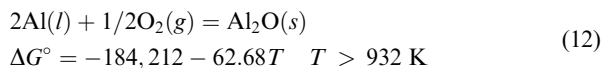
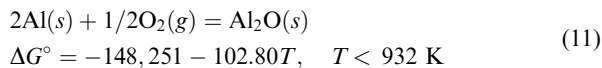
(a)			
T ($^{\circ}\text{C}$)	T (K)	τ_{id} (ks)	
600	873	1861.47	
700	973	160.79	
800	1073	54.02	
(b)			
T ($^{\circ}\text{C}$)	T (K)	τ_{pd} (ks)	
950	1223	35.95	
1100	1373	28.55	
1250	1523	23.02	
(b)			
T ($^{\circ}\text{C}$)	T (K)	τ_{id} (ks)	τ_{ca} (ks)
600	873	964.76	36.66
700	973	109.88	16.87
800	1073	28.18	7.88
(b)			
T ($^{\circ}\text{C}$)	T (K)	τ_{pd} (ks)	τ_{ca} (ks)
950	1223	23.08	2.54
1100	1373	18.27	1.71
1250	1523	16.17	1.10

into a solely rate-controlling process. According to the experimental results, the interfacial interaction of aluminum and its compounds with graphite totally eliminates the chemisorption step from the oxidation mechanism in MgO–C–Al bricks.

Figure 3 compares oxidized and nonoxidized regions of the XRD patterns of the MgO–C–Al probes before and after oxidation. The formation of carbide, nitride, and spinel phases at core–shell interfaces during oxidation experiments may be recognized from the emergence and growth of the associated peaks. Based on previous studies, formation of these compounds can affect pore geometry and carbon distribution within the unoxidized and oxidizing regions.^{12,21,22,31–34}

Aluminum compounds have a higher specific volume than the base refractory material.^{4,32,35–37} The formation of a number of these compounds is thermodynamically feasible at all temperatures. Al_4C_3 is practically produced at temperatures greater than 750°C .^{21,22} This compound results in MgO/graphite binding and reduction of brick permeability.³³ Formation of aluminum compounds due to a reaction between aluminum, carbon, nitrogen, oxygen, and the refractory materials is accompanied by an increase in the specific volume and seems to result in partial filling of the refractory micropores and reduction of the interdiffusion rate of the gases through the solid and porous regions of the oxidized shell.^{36–38}

In the presence of air, aluminum may also oxidize to Al_2O_3 .^{3,39}



The gases can migrate toward the cave nozzles and oxidize with the incoming oxygen to produce Al_2O_3 .^{40–42} $\text{MgO} \cdot \text{Al}_2\text{O}_3(s)$ spinel can also form by the reaction of $\text{Al}_2\text{O}_3(s)$ with $\text{MgO}(s)$:⁴³

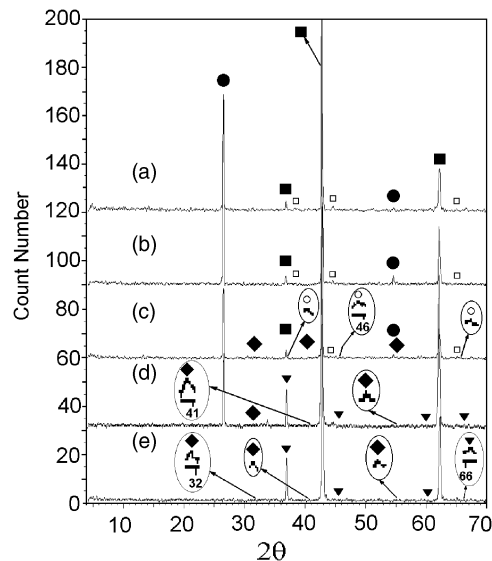
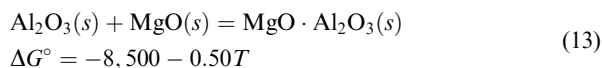
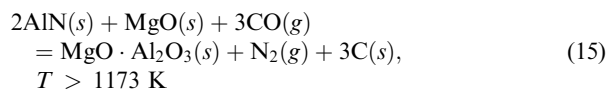
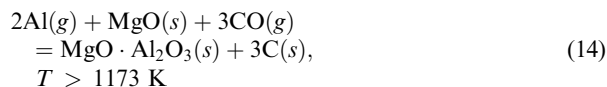


Fig. 3. X-ray diffraction pattern of MgO–C–Al refractory bricks: (a) before oxidation, (b) after oxidation at 600°C , (c) unreacted core after oxidation at 1250°C , (d) reaction interface after oxidation at 1250°C , and (e) reacted shell after oxidation at 1250°C . Patterns are shifted (a) 120, (b) 90, (c) 60, and (d) 30 counts upward. Highlighted peaks belong to trace compounds. They have been magnified 4 times. The symbols used denote: ■, MgO; ●, C; ◆, Al_4C_3 ; ○, AlN; □, Al; ▼, MgAl_2O_4 .



Practically, $\text{MgO} \cdot \text{Al}_2\text{O}_3(s)$ spinel forms at temperatures greater than 900°C . Its formation can also occur via the following reactions^{40,43}:



Spinel formation results in solid volume expansion, apparent porosity reduction, and pore-filling effects, which cause diminution of the effect of the competing chemical adsorption. Optical microscope and SEM images of the unreacted and reacted probes indicate morphological changes due to the aluminum addition and aluminum compound formation reactions.

Figure 4 illustrates the Arrhenius plots of the oxidation reaction. Activation energies and frequency factors of the oxidation reactions are obtained from slopes and intercepts of the $\ln(1/\tau)$ versus $1/T$ plots. The sharp change in slopes of the curves at 800°C indicates the variation of the cylindrical pore diffusion mechanism to solid-phase diffusion around flat graphite flakes. The reasons behind the occurrence of this process in aluminum-free refractory samples have been discussed elsewhere.¹ Similar reasons seem valid in aluminum-containing refractory probes. The only difference seems to be in the pore-filling constituent changes.

Close activation energies obtained for solid and pore interdiffusion of gases into both aluminum-containing and aluminum-free refractory bricks indicate similar diffusion mechanisms occurring in both cases. The adsorption step is, however, eliminated due to aluminum and aluminum compounds' catalytic behavior.³⁰ The data obtained from Arrhenius plots are used to determine the rate equations of the oxidation reactions. The

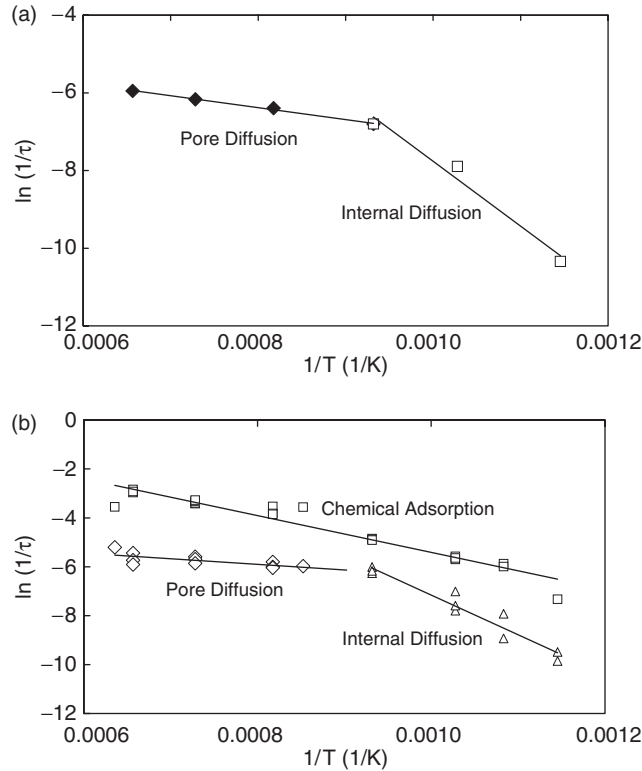


Fig. 4. Arrhenius plots of the oxidation reaction: (a) MgO-C-Al and (b) MgO-C. Note that total conversion times are expressed in minutes.

results are summarized in the following oxidation time versus fractional conversion equations:

$$\text{For MgO - C - Al at } T \leq 1073 \text{ K} \\ \Rightarrow t = \frac{1}{7929 \exp(-\frac{16738}{T})} x^2 \quad (16)$$

$$\text{For MgO - C - Al at } T \geq 1073 \text{ K} \\ \Rightarrow t = \frac{1}{0.02 \exp(-\frac{3064.6}{T})} [x + (1-x)\ln(1-x)] \quad (17)$$

$$\text{for MgO - C at } T \leq 1073 \text{ K} \\ \Rightarrow t = \frac{1}{8653 \exp(-\frac{16221}{T})} x^2 \\ + \frac{1}{8.25 \exp(-\frac{7521.9}{T})} x \quad (18)$$

$$\text{For MgO - C at } T \geq 1073 \text{ K} \\ \Rightarrow t = \frac{1}{0.02 \exp(-\frac{2298.1}{T})} [x + (1-x)\ln(1-x)] \\ + \frac{1}{8.25 \exp(-\frac{7521.9}{T})} x \quad (19)$$

Typical experimental data are compared with the model data for MgO-C probes in Fig. 5. Fractional weight changes obtained from Eqs. 18-19 are compared with the empirical data for oxidation of MgO-C-Al refractory bricks in Fig. 7. The results indicate that the rate of oxidation of the refractory bricks slightly increases below 750°C, but largely decreases at 800°-1250°C with aluminum addition. Based on previous studies,^{21,22} the oxidation rate-lowering effect of aluminum starts at 750°C. At higher temperatures, Al(g) penetrates into the MgO bricks and reacts with carbon and nitrogen to form plate-like Al₄C₃(s) and whisker-like AlN(s) as well as Al₂O₃·MgO spinel, which are

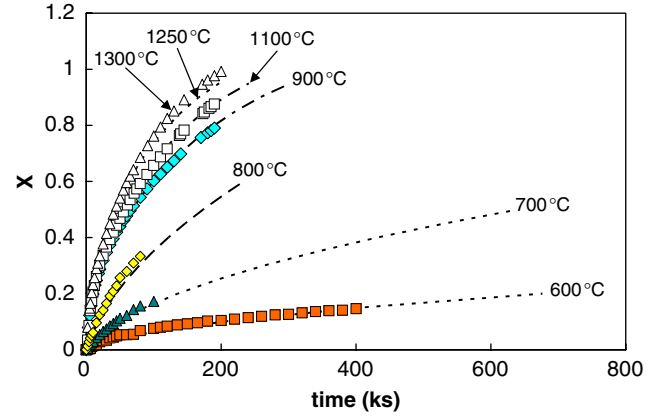
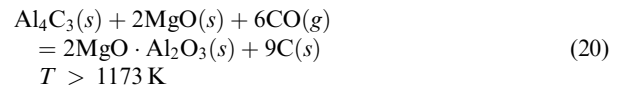


Fig. 5. Comparison of MgO-C experimental and calculated data. Symbols show the experimental results. Broken lines indicate the calculated data at the temperatures given.

accompanied by volume expansion, pore blockage, and protection against oxidation of refractory materials.^{11,21,22,43} The amount of spinel increases with temperature, especially when additional reactions involving conversion of Al₄C₃(s) come into play^{40,41}:



This process retards carbon loss due to oxidation.²¹⁻²³

The total amount of aluminum added is 1.5%, a fraction of which may be oxidized to Al₂O or Al₂O₃. Aluminum may, however, vaporize especially at temperatures greater than 1000°C. Figure 6 shows the equilibrium partial pressure of Al(g) as a function of temperature.⁴⁴ The weight change due to aluminum oxidation and vaporization must, of course, be considered in weight-loss calculations. The overall results seem, however, not too significant to dictate an absolute need for chemical analysis versus time of the oxidizing commercial MgO-C-Al sample. For simplicity, we ignored the possible role of aluminum oxidation/vaporization in weight change evaluations.

It seems that the formation of carbide and oxide phases at a higher temperatures ($T > 1000^\circ\text{C}$) causes a decrease of the apparent porosity and prevents oxidation of the graphite present in the refractory samples. This result is similar to what has previously been mentioned by other researchers.^{7-15,21}

Figure 7 shows a higher oxidation rate for MgO-C-Al than for MgO-C at 600° and 700°C. The lower porosity of MgO-C-Al samples dictates suppression of the rate of pore diffusion of oxygen toward the graphite flakes and their oxidation rate reduction. This is not, however, the case at these temperatures ($T < 800^\circ\text{C}$), because the oxidation of the samples does not follow a pore diffusion mechanism at these temperatures. It follows

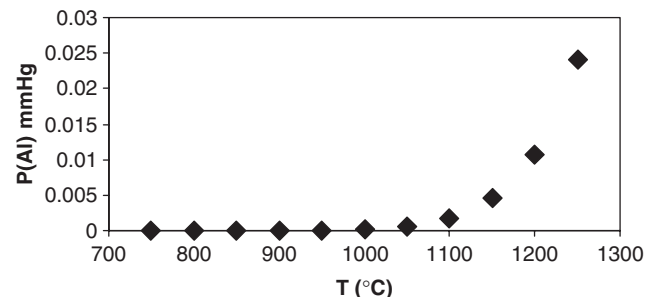


Fig. 6. Vapor pressure of aluminum against temperature.

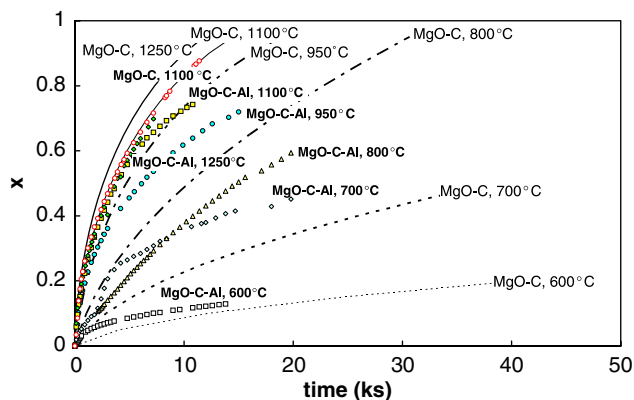


Fig. 7. Comparison of oxidation rate data for MgO-C-Al and MgO-C probes. Symbols show the experimental results; the solid and broken lines indicate the calculated data.

solid diffusion, which does not considerably change by densification. Aluminum removal of the chemisorption step plus its catalytic effect on graphite oxidation at $T < 800^\circ\text{C}$ brings about a shift in the weight-loss curves to higher fractions.³⁰

At higher temperatures $T \geq 800^\circ\text{C}$, pore diffusion prevails. Burning of carbon (both from soot and from flakes) increases porosity percentage in both MgO-C and MgO-C-Al samples. Pore blockage brought about by aluminum compounds yields, however, a lower porosity in MgO-C-Al probes as compared with MgO-C samples. As a result, the rate of oxidation of MgO-C-Al probes becomes lower than that of MgO-C samples. This results in the lowering of $x-t$ curves of MgO-C-Al as compared with MgO-C plots in Fig. 7.

Figure 7 indicates that weight-loss reduction due to aluminum addition at temperatures greater than 1100°C is lower than that at intermediate temperatures (e.g., $950^\circ\text{C} \geq T \geq 800^\circ\text{C}$). The higher amount of carbon oxidation results in a lower density and an increase in the extent and openness of the porous regions at these higher temperatures, which facilitates faster transfer of O_2 toward reaction sites and CO from reaction sites toward the exterior of the samples.

IV. Conclusions

1. The oxidation of an aluminum-free magnesia-graphite refractory is controlled by dual-step solid-phase diffusion/chemical adsorption at $T \leq 800^\circ\text{C}$ and dual-step pore diffusion/chemical adsorption at $T \geq 800^\circ\text{C}$.

2. The experimental data, combined with model calculations, indicate that in the presence of an Al antioxidant, the chemisorption step is totally eliminated. This phenomenon is attributed to the catalytic behavior of aluminum and its compounds, which facilitate the adsorption of oxygen to the surface of graphite flakes.

3. Addition of an aluminum antioxidant reduces the rate of oxidation of porous refractory bricks by production of voluminous compounds blocking the pore nozzles at intermediate temperatures between 800° and 1250°C , but increases the rate of oxidation of the refractory materials at 600° and 700°C by eliminating the chemical adsorption step and increasing the oxygen transfer rate to the surface of graphite flakes.

References

¹S. K. Sadrnezhaad, S. Mahshid, B. Hashemi, and Z. A. Nemat, "Oxidation Mechanism of C in MgO-C Refractory Bricks," *J. Am. Ceram. Soc.*, **89** [4] 1308–16 (2006).
²A. Watanabe, H. Takahashi, and F. Nakatani, "Mechanism of Dense Magnesia Layer Formation Near the Surface of Magnesia-Carbon Brick," *J. Am. Ceram. Soc.*, **69** [9] c-213–4 (1986).

³S. K. Sadrnezhaad, *Heat and Motion in Materials*. Foreign Ministry Press, Tehran, Iran, 1999 (ISBN 964-330-526-X).
⁴S. Zhang, N. J. Marriott, and W. E. Lee, "Thermochemistry and Microstructures of MgO-C Refractories Containing Various Antioxidants," *J. Eur. Ceram. Soc.*, **21** [8] 1037–47 (2001).
⁵A. Yamaguchi, "Effects of Oxygen and Nitrogen Partial Pressure on Stability of Metal, Carbide, Nitride, and Oxide in Carbon-Containing Refractories," *Taikabutsu Overseas*, **7** [1] 4–13 (1987).
⁶A. Yamaguchi, "Thermochemical Analysis for Reaction Processes of Aluminum and Aluminum Compounds in Carbon-Containing Refractories," *Taikabutsu Overseas*, **7** [2] 11–6 (1987).
⁷J. Poirier and M. A. J. Rigaud, "The Stability of Metals, Carbides and Oxides in Carbon-Magnesia Refractories," *Can. Ceram. Quart.*, **62** [1] 70–6 (1993).
⁸M. Subbanna, P. C. Kapor, and Pradio, "Role of Powder Size, Packing, Solid Loading and Dispersion in Colloidal Processing of Ceramics," *Ceram. Int.*, **28**, 401–5 (2002).
⁹M. Suzuki, H. Sato, M. Hasegawa, and M. Hirota, "Effect of Size Distribution on Tapping Properties of Fine Powders," *Powder Technol.*, **118**, 53–7 (2001).
¹⁰N. C. Lubaba, B. Rand, and N. H. Brett, "Compaction Studies of MgO-Flake Graphite Mixtures Relevant to the Fabrication of Composite Refractory Materials," *Br. Ceram. Trans.*, **87**, 158–63 (1988).
¹¹N. C. Lubaba, B. Rand, and N. H. Brett, "Microstructure and Strength of MgO-Carbon Composite Refractory Materials," *Br. Ceram. Trans.*, **88**, 47–54 (1989).
¹²S. C. Carniglia, "Limitation on Internal Oxidation-Reduction Reaction in BOF Refractories," *Am. Ceram. Soc. Bull.*, **52** [2] 160–5 (1973).
¹³K. Tabata, H. Nishio, and K. Itoh, "A Study on Oxidation-Reduction Reaction in MgO-C Refractories," *Taikabutsu Overseas*, **8** [4] 3–10 (1988).
¹⁴K. Ichikawa, H. Nishio, and Y. Hoshiyama, "Oxidation Test of MgO-C Bricks," *Taikabutsu Overseas*, **14** [1] 13–9 (1994).
¹⁵N. K. Ghosh, D. N. Ghosh, and K. P. Jagannatha, "Oxidation Mechanism of MgO-C in Air at Various Temperatures," *Br. Ceram. Trans.*, **99** [3] 142–8 (2000).
¹⁶M.-A. Faghghi-Sani and A. Yamaguchi, "Oxidation Kinetics of MgO-C Refractory Bricks," *Ceram. Int.*, **28**, 835–9 (2002).
¹⁷X. Li, M. Rigaud, and S. Palco, "Oxidation Kinetics of Graphite Phase in MgO-C Refractories," *J. Am. Ceram. Soc.*, **78** [4] 965–71 (1995).
¹⁸O. Levenspiel, *Chemical Reaction Engineering*. John Wiley, New York, 1972 (BN 0-471-53 016-6).
¹⁹B. Hashemi, Z. Ali Nemat, and S. K. Sadrnezhaad, "Oxidation Mechanisms in MgO-C Refractories," *China Refract.*, **13** [2] 13–20 (2004).
²⁰B. Hashemi, Z. Moghimi, Z. A. Nemat, and S. K. Sadrnezhaad, "Solid-Gas Reactions in MgO-C Refractories"; pp. 581–91 in *4th ISARIM-Symposium on Refractories*. Edited by M. Rigaud and C. Allaire. MET Society, Hamilton, Canada, 2004.
²¹Z. A. Nemat, S. K. Sadrnezhaad, and H. R. Ahmadi Moghari, "Effect of Ferrosilicon, Silicon and Aluminum Antioxidants on Microstructure and Mechanical Properties of Magnesia-Graphite Refractory," *Refract. Appl. News*, **10**, 2–9 (2005).
²²S. Uchida and K. Ichikawa, "High Temperature Properties of Unburned MgO-C Brick Containing Al and Si Powders," *J. Am. Ceram. Soc.*, **81** [11] 2910–6 (1998).
²³Y. Jitsumori, T. Yoshida, and A. Yamaguchi, "Effect of Starting Materials Characteristics on Microstructures and Properties of Magnesia Carbon Refractories," *Proceedings of the Unified International Technical Conference on Refractories*, Kyoto, Japan; 140–7 (1995).
²⁴E. Sereno and D. A. Brosnan, "Effect of Organic Fiber Additions on the Mechanical Properties of MgO-C Bricks," *Proceedings of the Unified International Technical Conference on Refractories*, New Orleans, LA; 775–82 (1997).
²⁵S. K. Sadrnezhaad, A. Gharavi, and A. Namazi, "Software for Kinetic Process Simulation," *IJE Trans. A: Basics*, **16** [1] 61–72 (2003).
²⁶N. Mazet and B. Spinner, "Modeling of Gas-Solid Reactions 2. Porous Solids," *Int. Chem. Eng.*, **32** [2] 271–84 (1992).
²⁷O. Levenspiel, *Chemical Reaction Engineering*, 2nd edition, John Wiley, New York, NY, 1972.
²⁸R. W. Mises and C. A. Mims, *Introduction to Chemical Reaction Engineering and Kinetics*, pp. 224–36. John Wiley and Sons Inc., New York, NY, 1999.
²⁹G. R. Doughty and L. S. Tovey, "A Comparison of the Oxidation Behavior in Air at 1050°C of Natural Flake Graphites," *Proceedings of the Unified International Technical Conference on Refractories*, Sao Paulo, Brazil; 830–9 (1993).
³⁰S. S. Zumdahl, *Chemistry*, 3rd edition, D. C. Heath and Company, Lexington, MA, 1993.
³¹K. Ichikawa, H. Nishio, O. Nomura, and Y. Hoshiyama, "Suppression Effects of Aluminum on Oxidation of MgO-C Bricks," *Taikabutsu Overseas*, **15** [2] 21–4 (1995).
³²X. Zhong, S. Hu and L. Dai, "Some Aspects in the Development of Steelplant Refractories in China," *Iron and Steel (China)*, **19** [7] 29–33 (1984).
³³H. Shikano, H. Tsutomu, H. Yamamoto, K. Tamaki, and T. Suruga, "Permeability of MgO-C Bricks," *Taikabutsu Overseas*, **11** [2] 32–3 (1991).
³⁴N. K. Ghosh, K. P. Jagannathan, and D. N. Ghosh, "Oxidation of Magnesia-Carbon Refractories with Addition of Aluminum and Silicon in Air," *Interceram*, **50** [3] 196–202 (2001).
³⁵A. Yamaguchi, S. Zhang, and J. Y. S. Hashimoto, "Behavior of Antioxidants Added to Carbon-Containing Refractories," *Proceedings of the Unified International Technical Conference on Refractories*, Kyoto, Japan; 341–8 (1995).
³⁶L. Hongxia, "Synthesis of New Composite Anti-Oxidants and their Application to Carbon Containing Refractories," *China's Refract.*, **9** [2] 3–6 (2000).

³⁷L. Kaiqi, "Refractories and Anti Oxidation Mechanism," *China's Refract.*, **9** [4] 18–20 (2000).

³⁸C. Baudin, C. Alvarez, and R. E. Moore, "Influence of Chemical Reaction in Magnesia–Graphite Refractories: II, Effects of Aluminum and Graphite Content in Generic Products," *J. Am. Ceram. Soc.*, **82** [12] 3539–48 (1999).

³⁹V. L. Lou, T. E. Mitchell, and A. H. Heuer, "Graphical Displays of the Thermodynamics of High-Temperature Gas–Solid Reactions and their Application to Oxidation of Metals and Evaporation of Oxides," *J. Am. Ceram. Soc.*, **68** [2] 49–58 (1985).

⁴⁰P. O. R. C. Brant and B. Rand, "Reactions of Silicon and Aluminum in MgO–Graphite Composites: I—Effects on Porosity and Microstructure," *Proceedings of the Unified International Technical Conference on Refractories*, 172–4 (1991).

⁴¹B. H. Baker and B. Brezny, "Dense Zone Formation in Magnesia–Graphite Refractories," *Proceedings of the Unified International Technical Conference on Refractories*, 168–71 (1991).

⁴²J. Ming-Xue, M. Ai-Qon, M. Xiang-Hong, and L. Yu-Ying, "A Thermodynamical Analysis of Reactions of Oxides with Carbon in Nitrogen Atmosphere," *Proceedings of the Unified International Technical Conference on Refractories*, Kyoto, Japan; 357–64 (1997).

⁴³Z. Dezhi and C. Shuxian, "The Effect of Additives on the Properties and Formation of MgO Dense Layer in MgO–C Permeable Samples," *Proceedings of the Unified International Technical Conference on Refractories*, Kyoto, Japan; 164–70 (1995).

⁴⁴O. Kubachewski and C. B. Alcock, *Metallurgical Thermochemistry*. Pergamon Press, USA, 1979. □